APPLICATION OF A FREQUENCY DOMAIN PRONY METHOD TO WIDE BANDWIDTH RADAR SIGNATURE CLASSIFICATION*

by

Rui J.P. de Figueiredo[+*] and C.L. Hu[+]

[+]Department of Electrical Engineering and
[*]Department of Mathematical Sciences
Rice University, Houston, Texas 77001

Technical Report EE 7908
September, 1979

*Supported by the RADC (Air Force Systems Command) Contract F 30602-78-C-0148 and the Office of Naval Research Contract N000 14-79-C-0442.

CONTENTS

SECURITY CLASSIFICATION OF THIS PAGE (When Data Entered)

REPORT DOCUMENTATION PAGE

READ INSTRUCTIONS BEFORE COMPLETING FORM

1. REPORT NUMBER: Rice Univ. Tech Report EE 7908	2. GOVT ACCESSION NO.
3. RECIPIENT'S CATALOG NUMBER	
4. TITLE (and Subtitle): APPLICATION OF A FREQUENCY DOMAIN PRONY METHOD TO WIDE BANDWITH RADAR SIGNATURE CLASSIFICATION	5. TYPE OF REPORT & PERIOD COVERED: Final
	6. PERFORMING ORG. REPORT NUMBER
7. AUTHOR(s): Rui J.P. de Figueiredo and C.L. Hu	8. CONTRACT OR GRANT NUMBER(s)
9. PERFORMING ORGANIZATION NAME AND ADDRESS: Dept. of Electrical Engineering, Rice University, Houston, Texas 77001	10. PROGRAM ELEMENT, PROJECT, TASK AREA & WORK UNIT NUMBERS
11. CONTROLLING OFFICE NAME AND ADDRESS: ISCP, Rome Air Development Center, Air Force Systems Command, Griffiss AFB, N. Y. 13441	12. REPORT DATE: September, 1979
	13. NUMBER OF PAGES: 28
14. MONITORING AGENCY NAME & ADDRESS (if different from Controlling Office)	15. SECURITY CLASS. (of this report): Unclassified
	15a. DECLASSIFICATION/DOWNGRADING SCHEDULE

16. DISTRIBUTION STATEMENT (of this Report)

APPROVED FOR PUBLIC RELEASE: DISTRIBUTION UNLIMITED

17. DISTRIBUTION STATEMENT (of the abstract entered in Block 20, if different from Report)

18. SUPPLEMENTARY NOTES

This work was also supported in part by the ONR Contract N000 14-79-C-0442

19. KEY WORDS (Continue on reverse side if necessary and identify by block number)

Fourier transforms; Prony approximation; Tauberian theorems; delayed signals; signal processing; radar signature processing; seismic signal processing.

20. ABSTRACT (Continue on reverse side if necessary and identify by block number)

A frequency domain Prony approach is presented for extracting features of return signals from targets illuminated by wide bandwidth (short pulse) radar. Theoretical details pertaining to this approach are described in a separate paper [1].

The features mentioned above consist of the relative delays and reflection coefficients pertaining to scattering centers on the target

DD FORM 1 JAN 73 1473 EDITION OF 1 NOV 65 IS OBSOLETE

SECURITY CLASSIFICATION OF THIS PAGE (When Data Entered)

representing differently shaped regions on the target surface. The dimensionality of the feature vectors thus constructed is very low (less than ten). Moreover, when used in the classification of targets by a nearest neighbor classification strategy, such feature vectors permit accurate discrimination between targets that do not differ much in shape; and also they are in a large measure insensitive to noise.

The above results were corroborated by computer simulations performed on the data base created by the coherent X-band short pulse (0.5 nanosecond) radar at the Fort Worth operation Radar Range of General Dynamics Convair Aerospace Division. The three objects on which extensive simulations were carried out were: an AGENA space vehicle with rectangular cross-sectional first stage, an AGENA space vehicle with cylindrical cross-sectional first stage and an AGENA space vehicle payload. The results of these simulations, which were rather sucessful, are discussed in detail.

[1] R.J.P.de Figueiredo and C.L. Hu, "A Fourier-Prony Tauberian Approach to the Analysis of a Mixture of Delayed Signals", Rice University Technical Report EE-7907, Houston, Texas, September 1979.

1. INTRODUCTION

In a wide bandwidth (short pulse) radar system*, the return signal consists of a sequence of short pulses emanating from different scattering centers on the target [2, 3, 4, 5]. These centers represent differently shaped regions on the target surface. Figure 1 illustrates

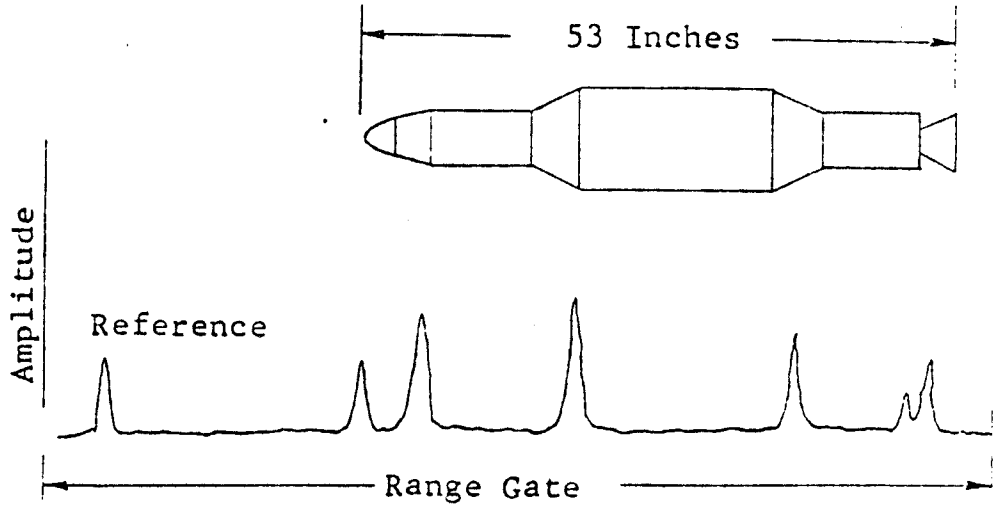

Fig. 1 Typical Short-Pulse Signature

the X-band radar return signature from 1/8-scale model of an AGENA vehicle taken from reference [3]. The first pulse is the return from a fixed reference scatterer, while the remaining pulses occur at the points of discontinuities on the vehicle surface as shown.

*Wide bandwidth radar systems are of recent vintage and possess the very high resolution needed to identify complex objects. Examples of such systems are the SPTF facility at Floyd, New York and the ARPA-Lincoln ALCOR facility at Kwajalean.

In what follows, we use a Tauberian representation for the return signal y, that is

$$y(t) = \sum_{i=1}^{M} a_i \, x(t - \tau_i), \tag{1}$$

where x is the reference pulse, shaped as the incident pulse, and a_i and τ_i are the reflection coefficient and delay associated with the ith scatterer. In the more general case in which the scatterers are distributed over the larger surface, we have a representation for y in the form

$$y(t) = \int_0^t h(t - t') \, x(t') \, dt', \tag{2}$$

where

$$h(t) = \sum_{i=1}^{M} a_i \, \Phi(t - \tau_i - \tau_0) \tag{3}$$

is the impulse reponse of the target; and τ_0 is the delay corresponding to the target range.

Let the data consist of a set of samples $x_n \triangleq x(t_0 + n \, \Delta t)$ and $y_n \triangleq y(t_0 - \tau_0 + n \, \Delta t)$, n = 0, 1, ..., N-1, of x and y, where the constants t_0, τ_0, and Δt are conveniently chosen. In the present paper, we propose the use of a frequency domain Prony approach, discussed in detail elsewhere [1], to determine the parameter vectors $\underline{\tau} = (\tau_1, \ldots, \tau_M)$ and $\underline{a} = (a_1, \ldots, a_M)$, from the above data. One can then use an appropriate subset of the variables $a_1, \tau_1, a_2, \tau_2, \ldots, a_M, \tau_M$, and of the parameters in h_i, as the components of a feature vector w in a nearest neighbor algorithm for target classification. In the present

paper, we limit our attention to the representation (1), the generalization to the case of equations (2) and (3) being clear from the developments in [1].

In section 2, we briefly describe the frequency domain Prony approach used here. In sections 3 and 4, we present the results of some of the simulations performed on the signature data obtained through use of the coherent, X-band short-pulse (0.5 nanosecond) radar at the Fort Worth operation Radar Range of General Dynamics Convair Aerospace Division. The data was provided to us on tape by the Rome Air Development Center (RADC) (Air Force Systems Command). Specifically we are concerned, in section 3, with the properties of the Tauberian representation (1), and, in section 4, with the application of the nearest neighbor algorithm for target classification using a few of the components of $\underline{a}$ and $\underline{\tau}$ as features. Using in some cases not more than 8 features and not less than four features, accurate discrimination among three space vehicles was achieved.

2. THE FREQUENCY DOMAIN PRONY ALGORITHM

The application of the frequency domain Prony algorithm for analysis of the return signature for short pulse radar was first considered by H. Webb [6] and E. M. Kennaugh [7]. Frequency domain Prony methods for both noise-free and noisy data were investigated in detail by the authors in [1].

To apply the Prony technique to equation (1), we simply take the Fourier transform of (1) to obtain

$$H(\omega) = \frac{Y(\omega)}{X(\omega)} = \sum_{i=1}^{M} a_i e^{-j \tau_i \omega}. \tag{4}$$

From the smaples $x_0, \ldots, x_{N-1}$, and $y_0, \ldots, y_{N-1}$, one calculates by DFT a set of samples of H at equidistant frequency points $\omega_k = \omega_0 + k \Delta\omega$, $k = 0, \ldots, K - 1$, where $2M \leq K \leq N$.

Let us use the notation

$$H_k = H(\omega_k). \tag{5}$$

We use the Prony algorithm to find the 2M parameters in the vectors $\underline{\tau} = (\tau_1, \ldots, \tau_M)$ and $\underline{a} = (a_1, \ldots, a_M)$ by fitting the complex numbers H_k, calculated from the data, to the expression (4), with equality or in the least squares sense, i.e.,

$$\sum_{i=1}^{M} a_i e^{-j \tau_i \omega_k} = H_k, \quad k = 0, 1, \ldots, K-1. \tag{6}$$

A modification of the conventional Prony method to conveniently take care of the fact that H_k are complex-valued (rather than real valued as in the conventional case) is presented in [1]. We have also shown in [1] how to apply our procedure when the smaples are noisy and also how to take care of the general case of the expressions (2) and (3) using Prony techniques. In the present paper we do not discuss these developments and simply assuming that the return signal has the form (1), and given the samples of x and y, we determine $\underline{\tau}$ and $\underline{a}$ by the procedure mentioned.

We now proceed to explain our approach to radar signature classification in the context of simulation results performed both on noiseless and noisy data.

3. TAUBERIAN RECONSTRUCTION OF THE RETURN SIGNAL

The actual radar return signal $\tilde{y}$ consists of samples of a frequency carrier in the X-band, single-sideband modulated by the scatterer interaction. Hence $\tilde{y}$ has the form

$$\tilde{y}(n) = \alpha(t_o - \tau_o + n\,\Delta t)\cos\omega_o(t_o - \tau_o + n\,\Delta t)$$
$$+\beta(t_o - \tau_o + n\,\Delta t)\sin\omega_o(t_o - \tau_o + n\,\Delta t)$$
$$n = 0, 1, \ldots, N-1, \qquad (7)$$

where ω_o denotes the carrier frequency, and $\alpha(\cdot)$ and $\beta(\cdot)$ are functions representing the modulation. By passing $\tilde{y}$ through a synchronous detector system such as the one shown in Figure 2, the envelope and phase information in terms of the variables y_n and θ_n are defined by (8a) and (8b);

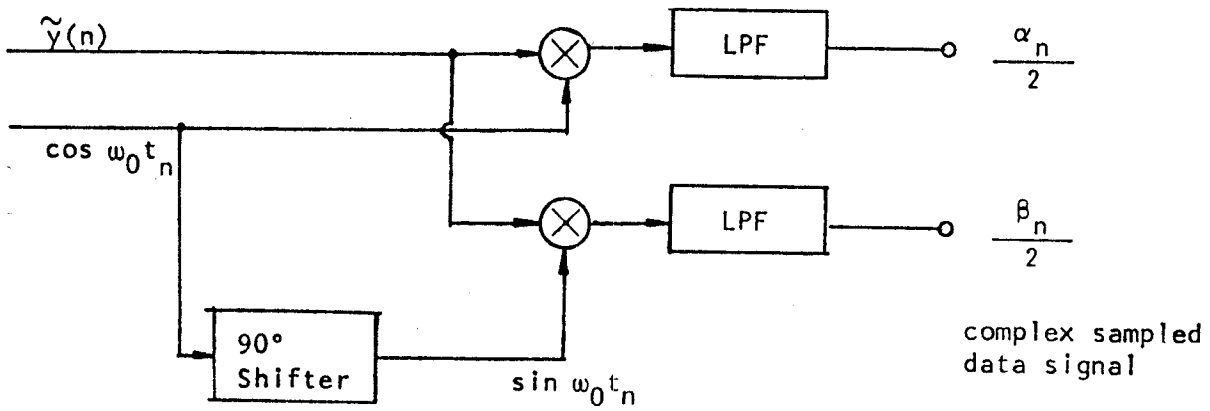

$$t_n = t_0 - \tau_0 + n\Delta t$$
$$\alpha_n = \alpha(t_n)$$
$$\beta_n = \beta(t_n)$$

Fig. 2 Synchronous Detection System

$$y_n = y(t_0 - \tau_0 + n\,\Delta t) = \sqrt{\alpha^2(t_0 - \tau_0 + n\,\Delta t) + \beta^2(t_0 - \tau_0 + n\,\Delta t)}, \tag{8a}$$

$$\theta_n = \theta(t_0 - \tau_0 + n\,\Delta t) = \tan^{-1}[\beta(t_0 - \tau_0 + n\,\Delta t)/\alpha(t_0 - \tau_0 + n\,\Delta t)],$$

$$n = 0, \ldots, N-1 \tag{8b}$$

The phase sequence $\{\theta_n\}$ was not used in our classification algorithm. For each space vehicle model investigated, the envelope sequence $\{y_n\}$ for a given yawing angle was obtained from tapes supplied to us by RADC. The reference pulse (the first pulse in Figure 1) was used as the waveform of x.

Our first set of simulations, described in the present section, were designed to test the representation (1) by reconstructing the actual waveform y as the waveform $\hat{y}$ described by

$$\hat{y}(n) = \sum_{i=1}^{M} a_i\, x(n - \tau_i) \tag{9}$$

where the constants a_i and τ_i were calculated by fitting the data $\{y_n : n = 0, \ldots, N-1\}$ and $\{x_n : n = 0, \ldots, N-1\}$ to the expression (1) by our frequency domain Prony technique, i.e. we calculated H_k by

$$H_k = \frac{\sum_{n=0}^{N-1} Y_n\, e^{-j\omega_k n}}{\sum_{n=0}^{N-1} X_n\, e^{-j\omega_k n}}, \quad k = 0, 1, \ldots, K-1 \tag{10}$$

and then obtained $\underline{\tau}$ and $\underline{a}$ by satisfying (6) using the Prony method. The number M of delays was set equal to an integer slightly greater than the number of peaks of high amplitude.

The data used is described in the reports by Cisco, Johnston, and Gruver [2], Cisco, Coble, and Gruver [3].

In our simulations we selected as targets the following three

objects at yawing angles indicated:

Model 59: AGENA space vehicle with rectangular cross-sectional first stage, yawing angle $\theta = 0.2^0$;

Model 66: AGENA space vehicle with cylindrical cross-sectional first stage, yawing angle $\theta = 0.2^0$;

Model 60: AGENA space vehicle payload, yawing angle $\theta = 31.2^0$.

For each case the demodulated radar return signal recorded in the tape is exhibited in Figures 3, 4, and 5 respectively. Figures 6, 7, and 8 show the locations of these signatures in 3-dimensional plots of intensity versus time and yawing angle (obtained from [2]).

We now comment on the reconstruction of the return signature for each of the above models separately.

Model 59:

We first removed the bias in the signature for this model (appearing in Figure 3)and selected for display in Figure 9 the useful sections of the signature, namely the reference signal x and the return y, side by side.

We assumed, first, the order (number of delays) M of the system to be 4, and applied the frequency domain Prony method to this data.

The signal $\hat{y}$ reconstructed according to (9) using the parameters $\underline{\tau}$ and $\underline{a}$ thus calculted is shown by the full curve of Figure 10 (the true signature y is represented by the dotted curve in this figure). The negative peak results from the physically unmeaningful fact that the parameter a_3 calculated above is negative. We concluded therefore that the third delay was redundant and reduced M to 3, and applying the same procedure, obtained the values for $\underline{\tau}$ and $\underline{a}$ tabulated in Table 1 in the

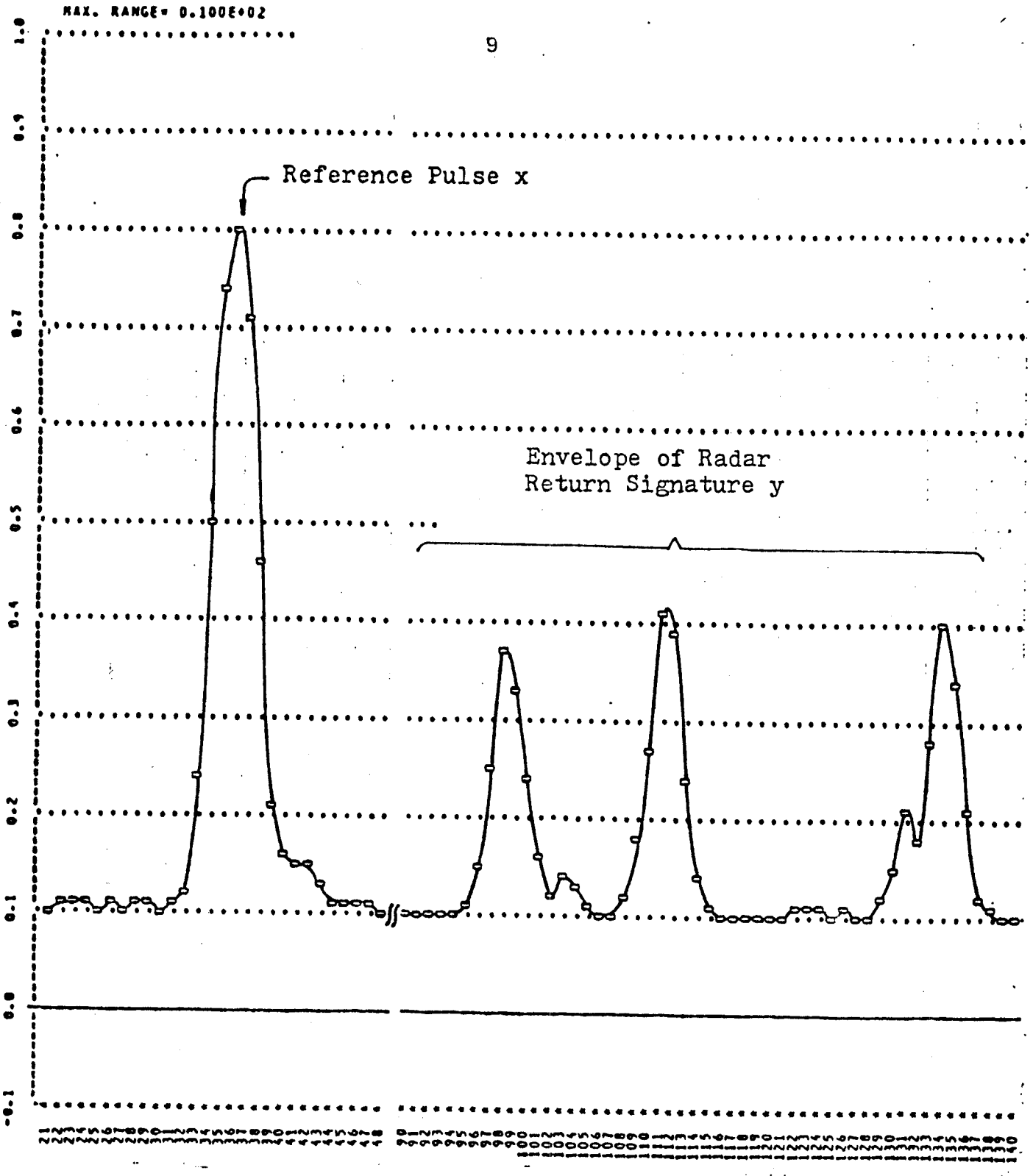

Fig. 3 The Reference Signal x and the Return y for Model 59 at Yawing Angle 0.2 degree

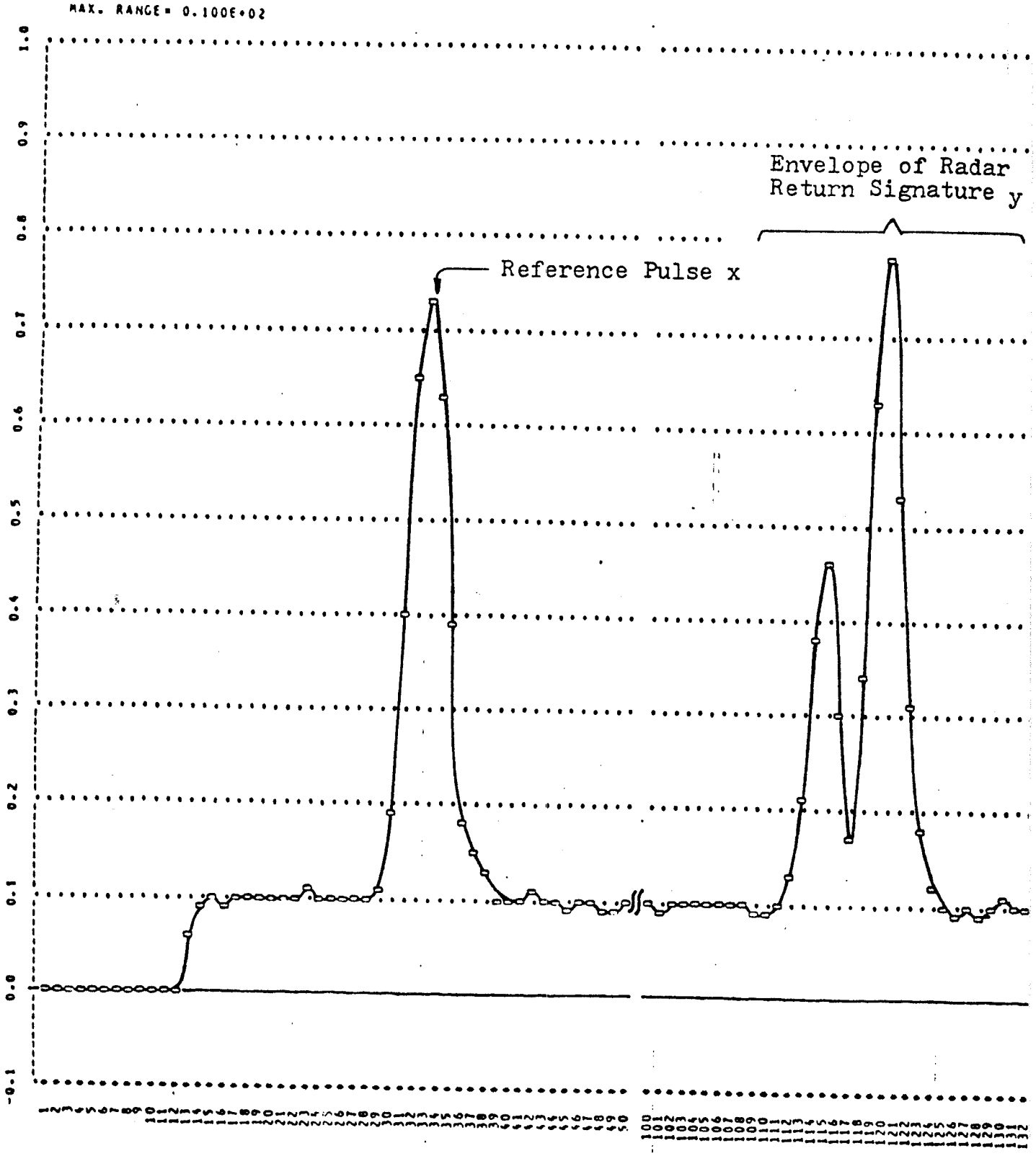

Fig. 4 The Reference Signal x and the Return y for Model 66 at Yawing Angle 0.2 degree

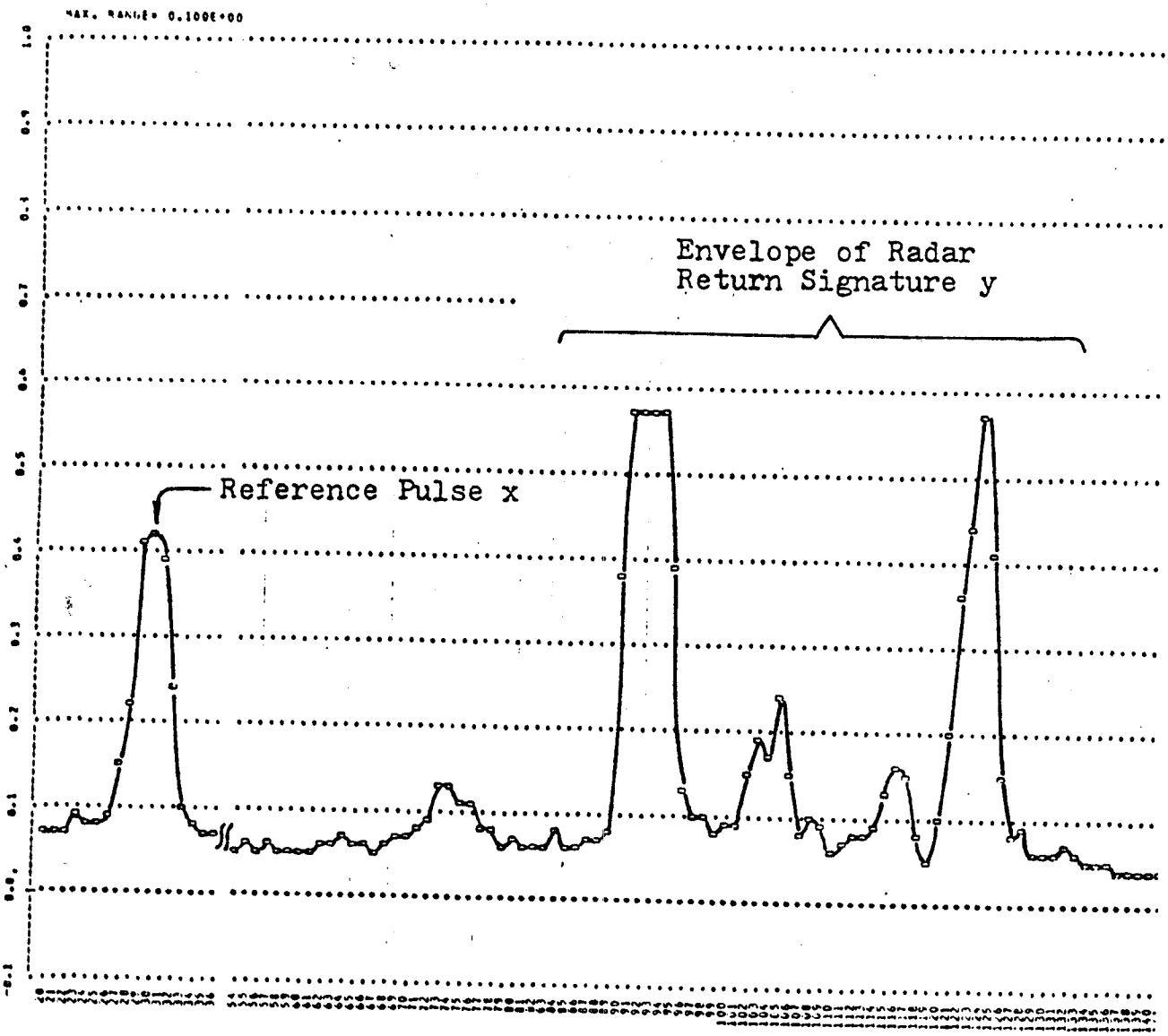

Fig. 5 The Reference Signal x and the Return y for Model 60 at Yawing Angle 31.2 degrees

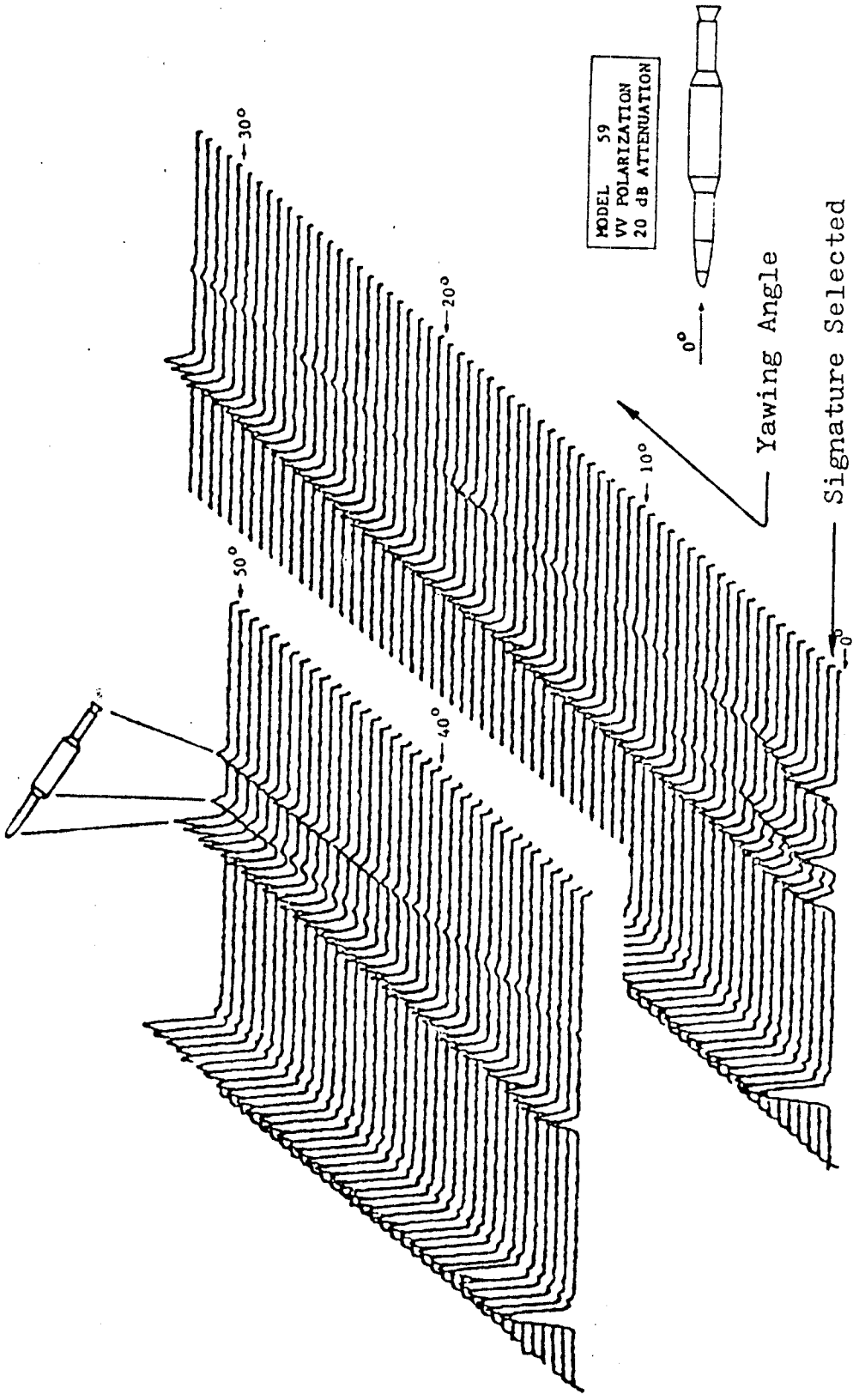

Fig. 6 Response of Aerospace Model 59

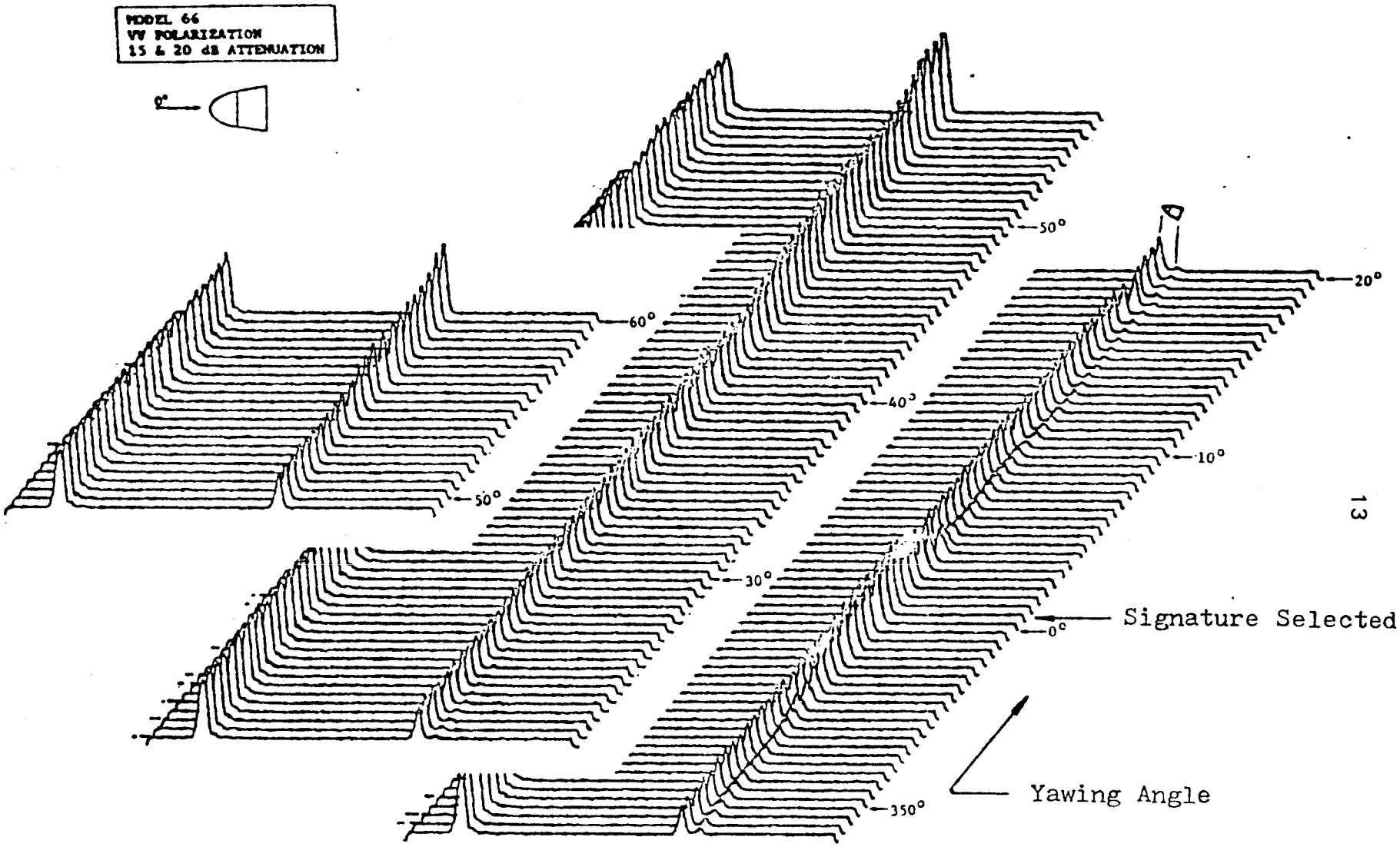

Fig. 7 Response of Aerospace Model 66

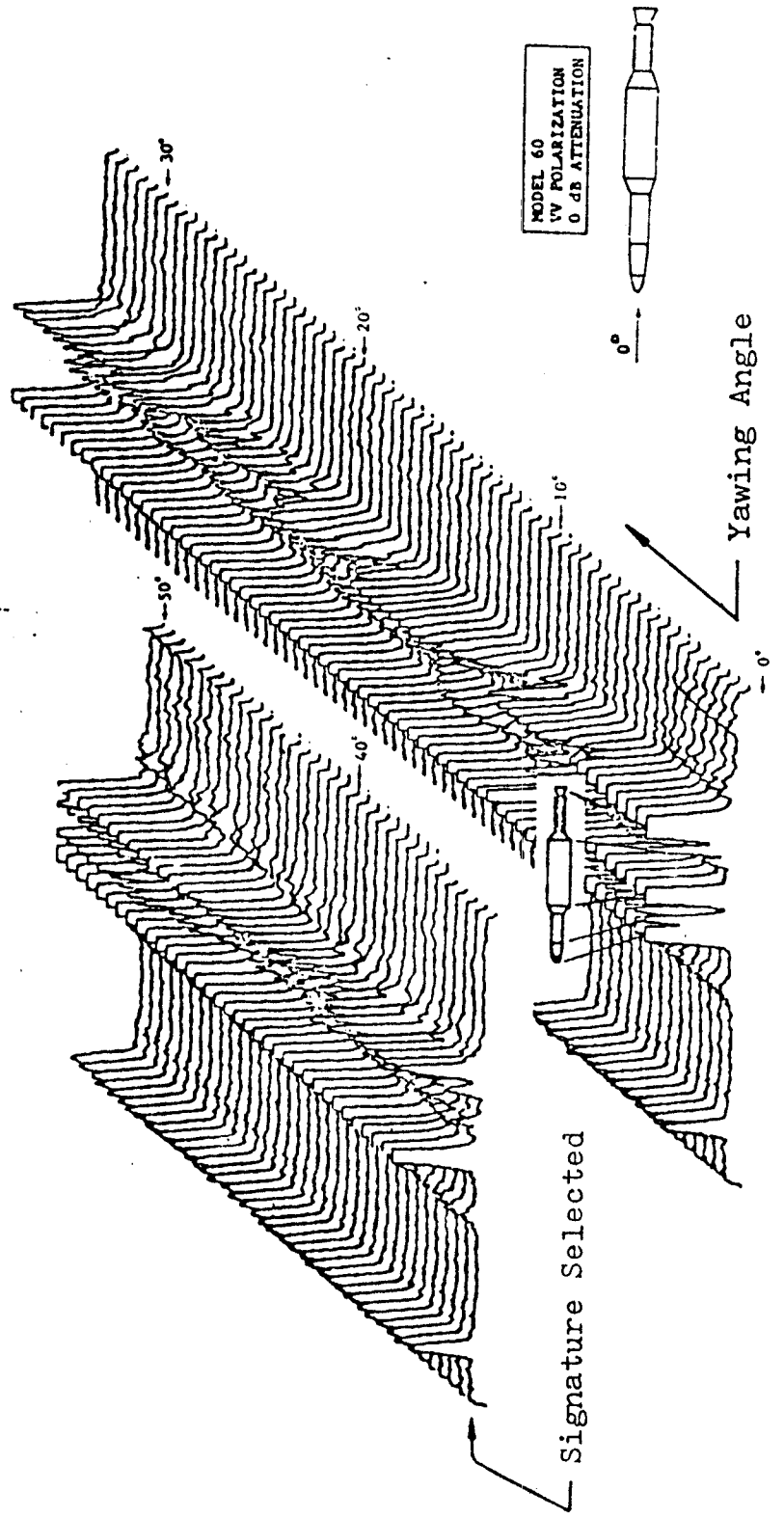

Fig. 8 Response of Aerospace Model 60

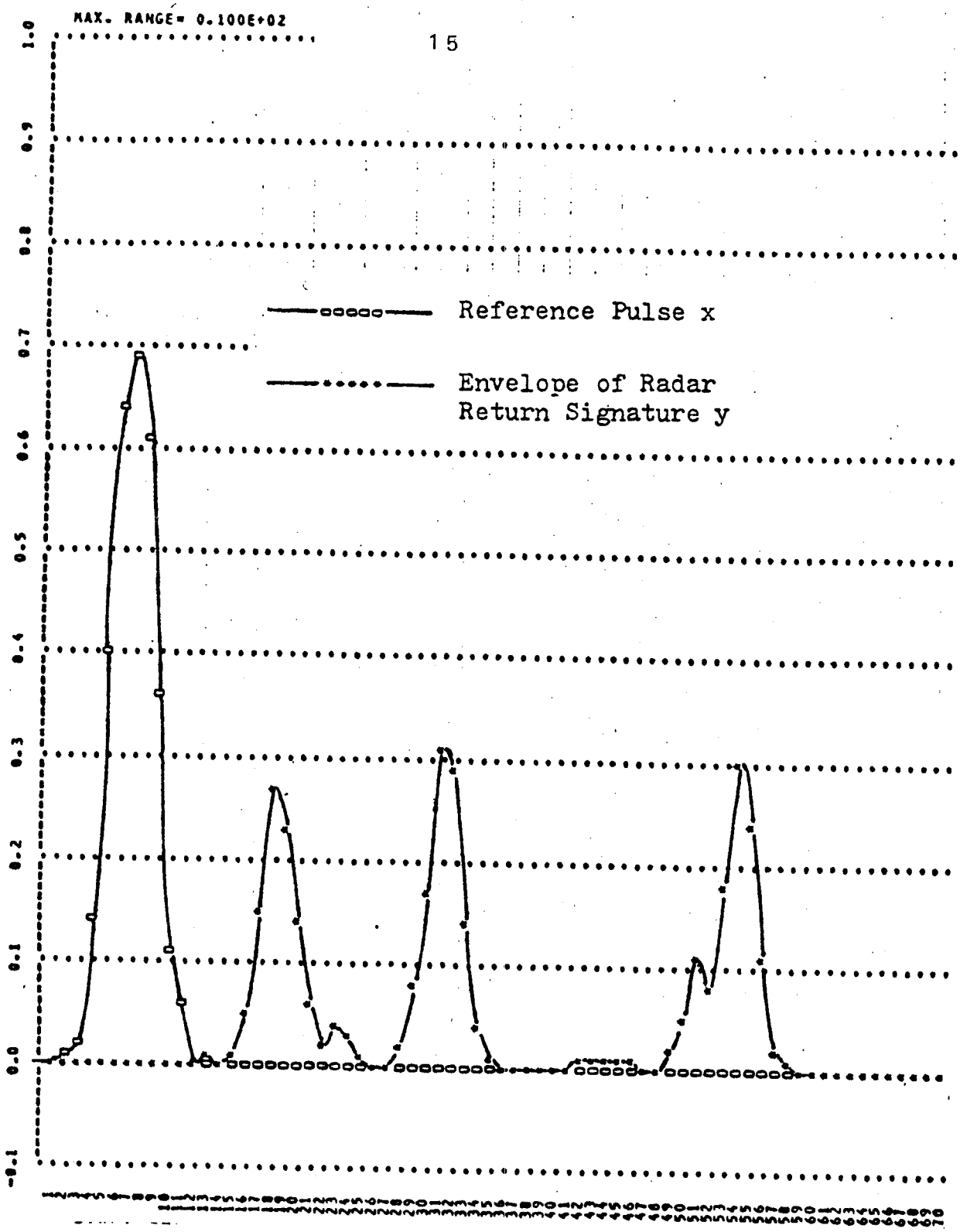

Fig. 9 The Corrected Signatures x and y for Model 59 at Yawing Angle 0.2 Degree

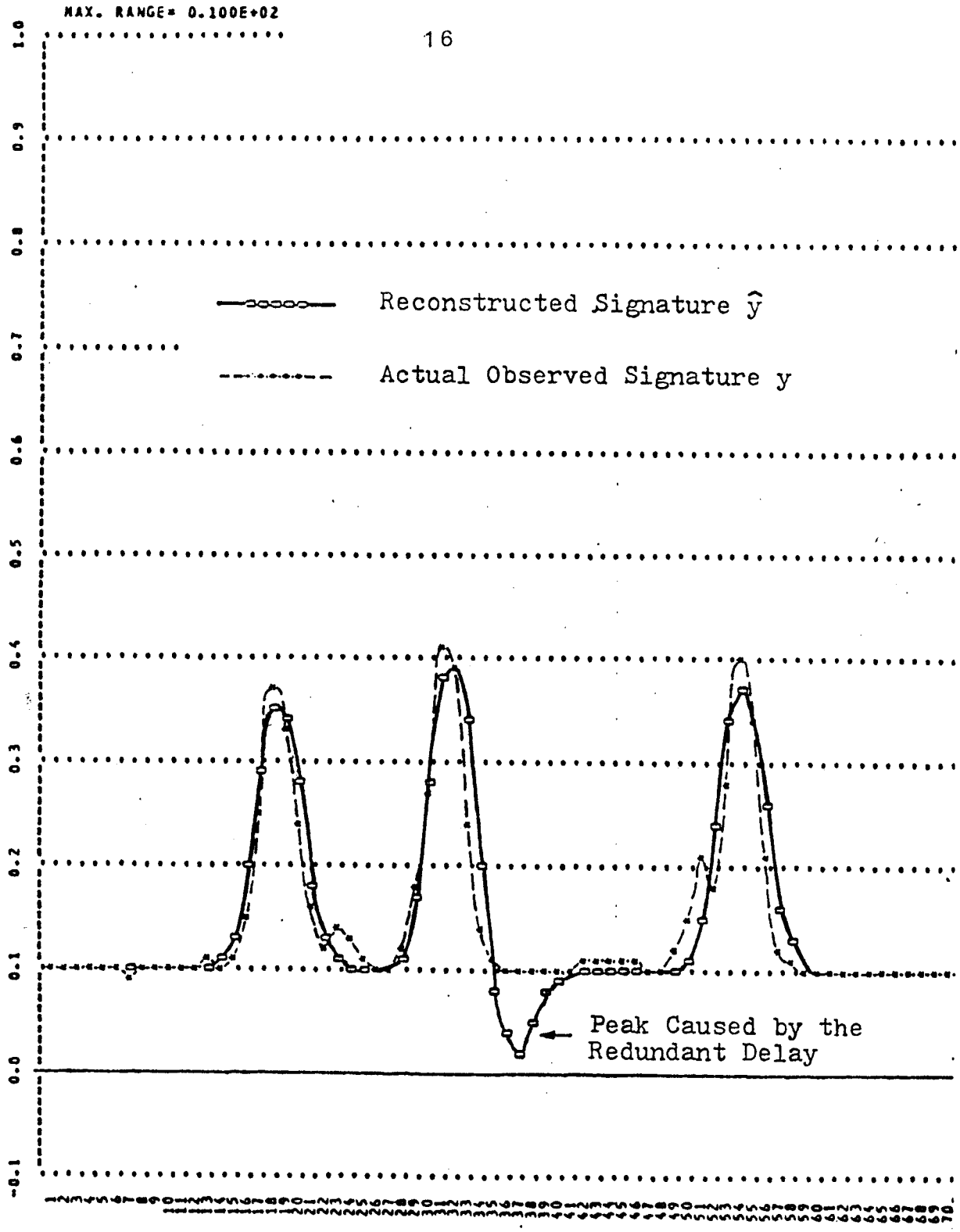

Fig. 10 Comparison of the Actual Observed Signature with the Reconstructed Signature for Model 59 at Yawing Angle 0.2 Degree

row labeled "Model 59: clean data".

The waveform reconstructed by means of these parameter vectors is shown by the full curve of Figure 11. We note that it agrees very closely with the actual signature shown by the dotted curve.

Model 66 and 60:

The delay and coefficient vectors $\underline{\tau}$ and $\underline{a}$ were calculated in the same way as for the model 59, they are listed in the rows of Table 1 labeled as clean data for these two models. The corresponding reconstruction $\hat{y}$ of the signal y is shown respectively in Figures 12 and 13.

Table 1

Model 59 at $\theta=0.2^0$	Clean Data	Delays	11.4765	24.9251	47.1603	
		Amps	0.3699	0.4304	0.3935	
	Noisy Data	Delays	11.3001	25.3624	47.1058	
		Amp	0.3794	0.5373	0.3673	
Model 60 at $\theta=31.2^0$	Clean Data	Delays	5.0879	24.4645	37.7121	55.9327
		Amps	0.1661	1.7065	0.3537	1.2050
	Noisy Data	Delays	4.4692	24.6126	38.0665	56.5352
		Amps	0.0177	1.8748	0.3418	1.2164
Model 66 at $\theta=0.2^0$	Clean Data	Delays	17.4324	23.1708		
		Amps	0.5375	0.9985		
	Noisy Data	Delays	17.3490	22.9287		
		Amps	0.6203	0.9188		

In order to test the robustness of our procedure, we contaminated the data with additive white Gaussian noise with zero mean and signal-to-noise ratio equal to 7.75. The results of the application of our procedure modified for the noisy case according to the developments in [1] are shown in the rows of Table 1 labeled as pertaining to noisy data. We note that there is very little change in the parameter values due to noise.

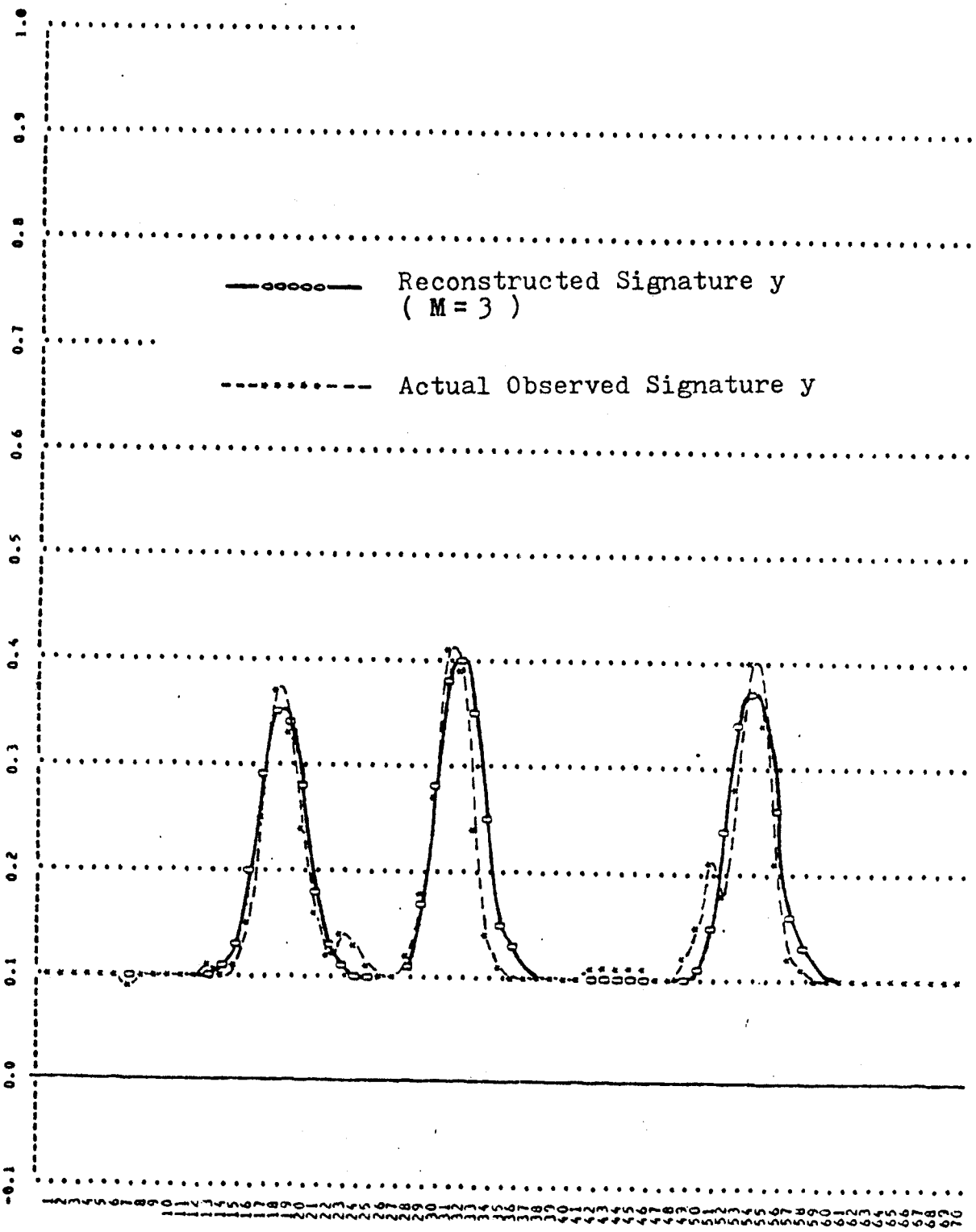

Fig. 11 Comparison of the Actual Observed Signature with the Reconstructed Signature (M = 3) for Model 59 at Yawing Angle 0.2 Degree

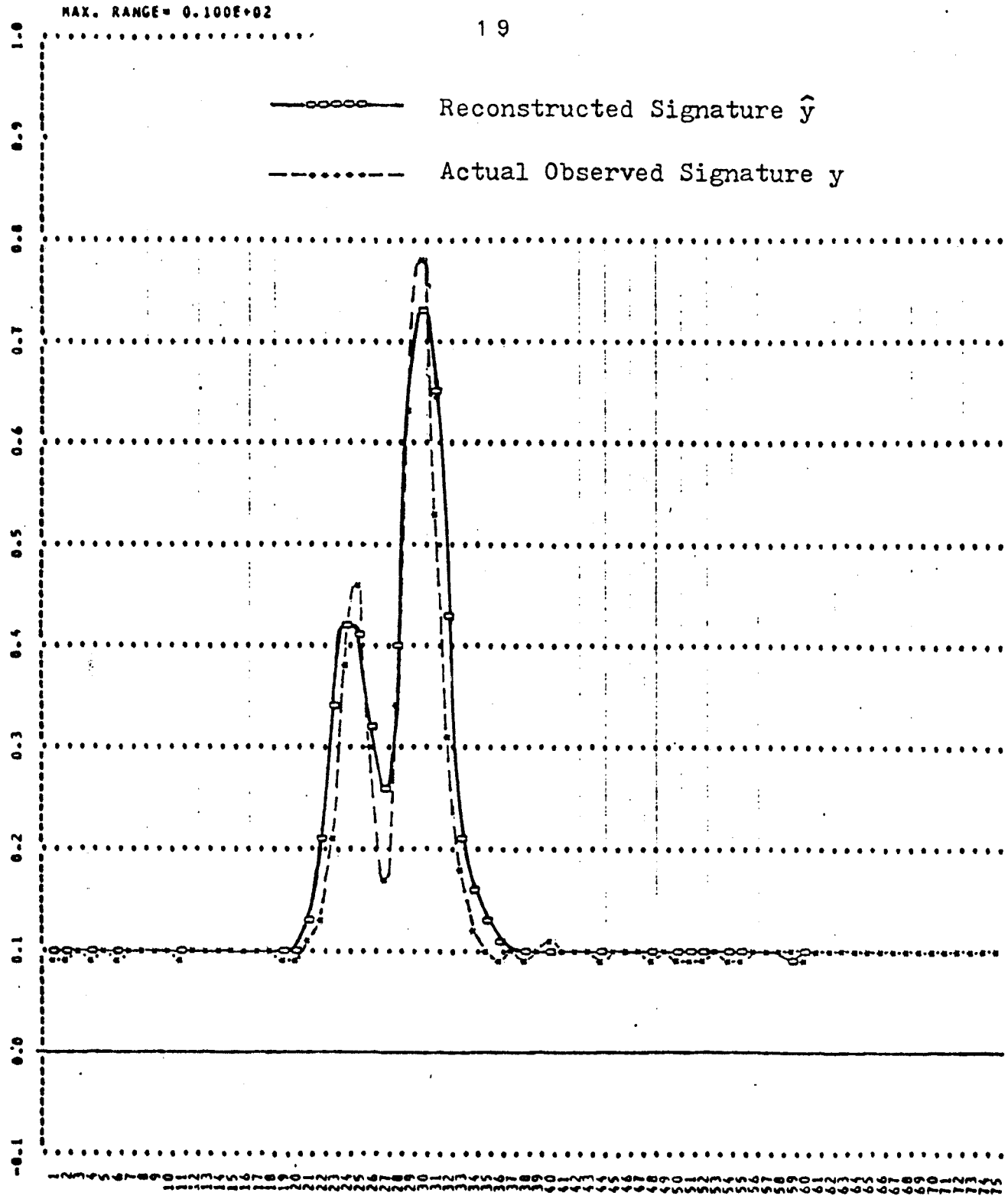

Fig. 12 Comparison of the Actual Observed Signature with the Reconstructed Signature for Model 66 at Yawing Angle 0.2 Degree

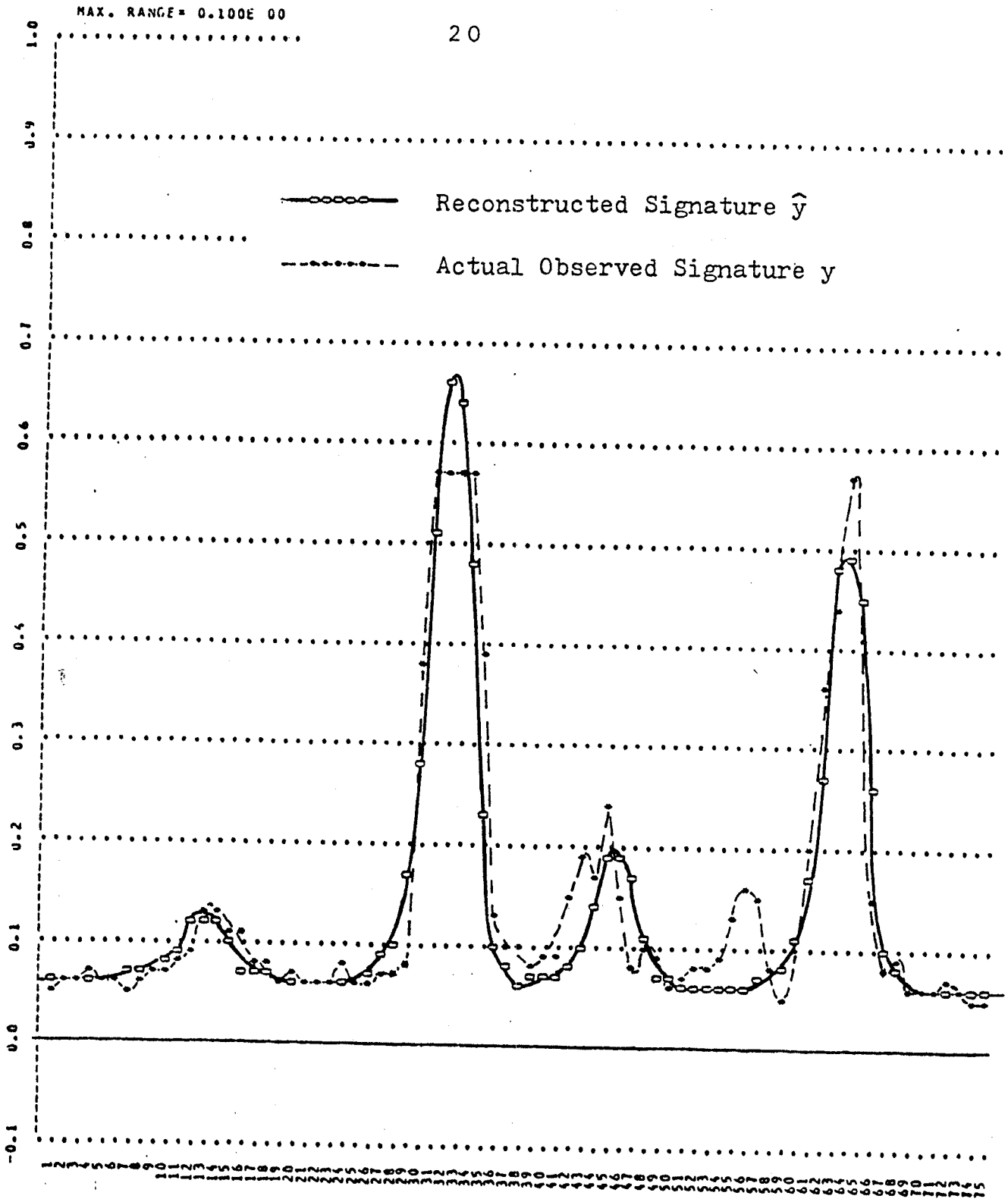

Fig. 13 Comparison of the Actual Observed Signature with the Reconstructed Signature for Model 60 at Yawing Angle 31.2 Degrees

For model 59, we further investigated the effect of noise on the calculated parameter values for different signal-to-noise ratios. The results are summarized in Table 2. Again, there is very close agreement between the corresponding noise-free and noisy cases. These remarkably

Table 2

No Added Noise	Delays	11.4765	24.9251	47.1603
	Amps	0.3699	0.4304	0.3935
S/N=7.75	Delays	11.3001	25.3624	47.1058
	Amps	0.3794	0.5373	0.3673
S/N=3.88	Delays	11.0809	24.7749	47.5632
	Amps	0.3038	0.3922	0.3039
S/N=2.58	Delays	10.9414	24.8378	47.7400
	Amps	0.2947	0.3922	0.2801
S/N=1.94	Delays	10.8262	24.9027	47.9388
	Amps	0.2847	0.3979	0.2545
S/N=1.29	Delays	10.6595	25.0273	48.3992
	Amps	0.2658	0.4122	0.2000

good results are highlighted by the curves of Figure 14 and 15. In Figure 14 the reconstructed signature $\hat{y}$ with parameters calculated from noisy data, for signal-to-noise ratio = 1.29, is compared to the actual noisy signature (i.e. original signature with noise added). Figure 15 compares the same signatue $\hat{y}$ (reconstructed from the noisy data with signal-to-noise ratio = 1.29) to that reconstructed from clean data.

These simulations clearly attest to the good robustness of our procedure.

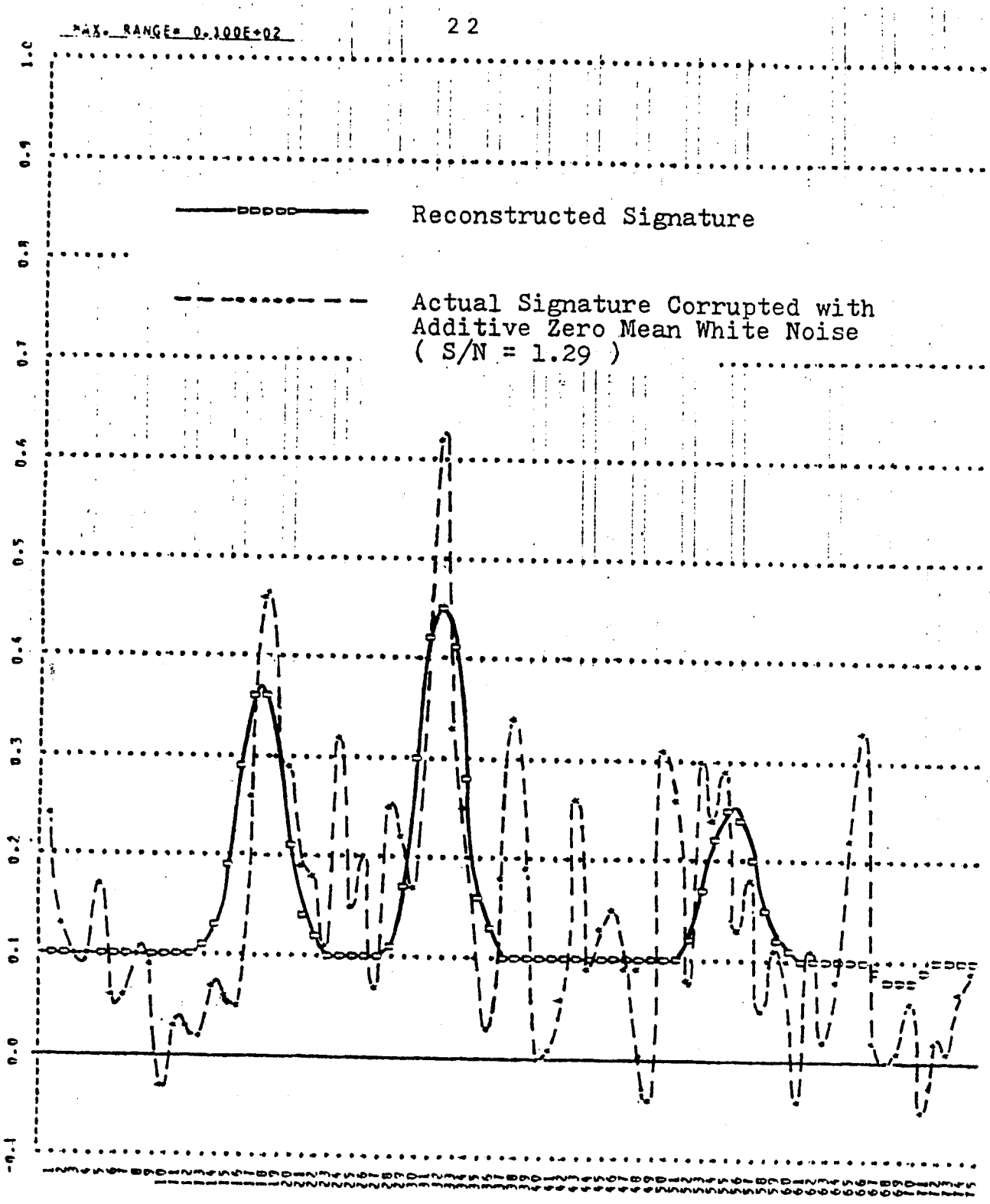

Fig. 14 Comparison of the Actual Noisy Signature with the Reconstructed Signature for Model 59 at Yawing Angle 0.2 Degree

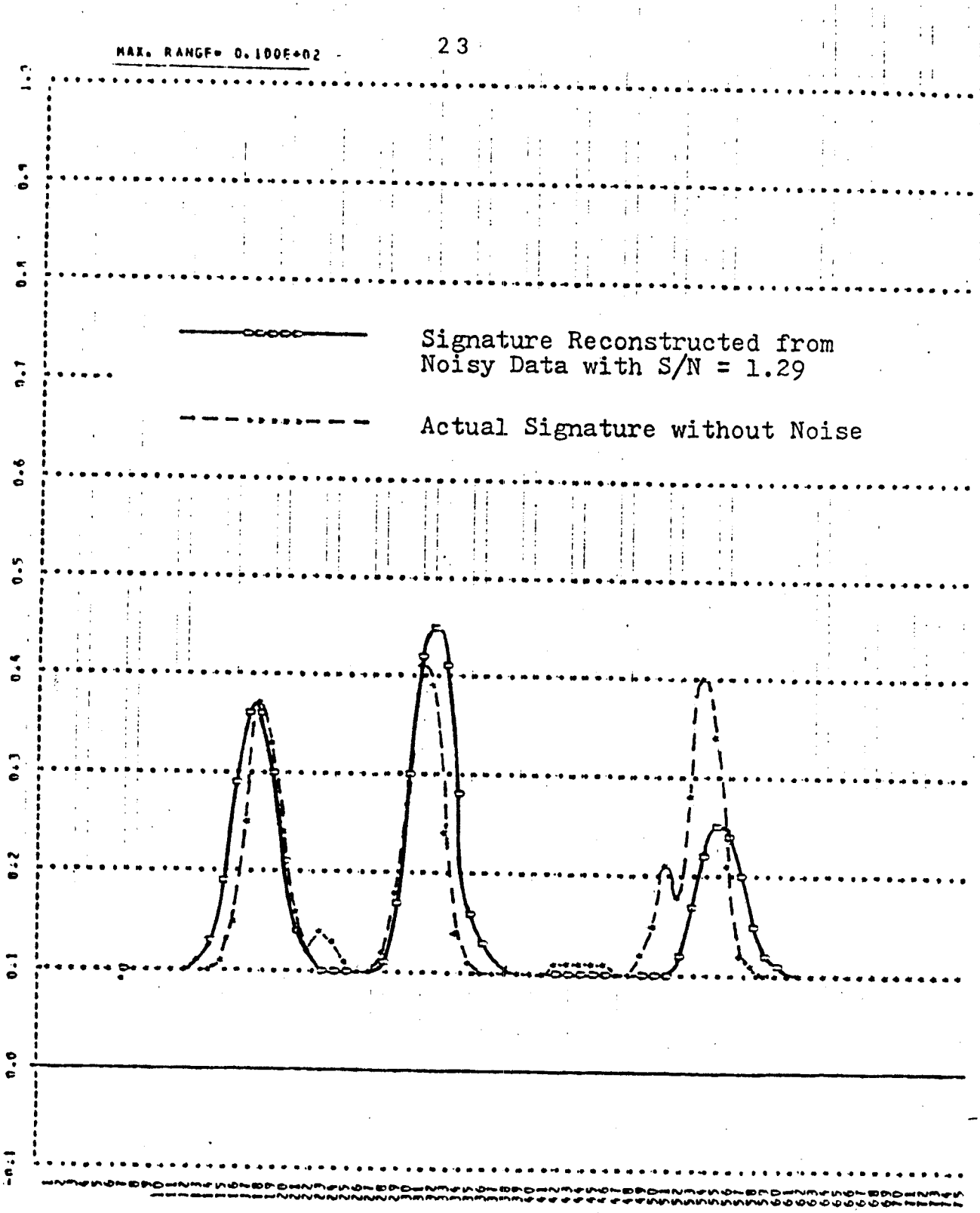

Fig. 15 Comparison of the Signature Reconstructed from Noisy Data with the Actual Signature without Noise for Model 59 at Yawing Angle 0.2 Degree

4. A PATTERN RECOGNITION ALGORITHM FOR RADAR RETURN SIGNATURE CLASSIFICATION

Suppose there are n standard models whose return signatures are known. Let $\underline{\tau}^i$ and $\underline{a}^i$ denote the parameter vectors $\underline{\tau}$ and $\underline{a}$ belonging to the ith model. Then we denote by M the dimension of the longest vector $\underline{\tau}^i$, $i = 1, \ldots, n$; and we change the lengths of all the vectors $\underline{\tau}^i$ and $\underline{a}^i$ to M using the convention that if the kth model has $\underline{\tau}$ of length $M_k < M$ then the first M_k entries of $\underline{\tau}^k$ will consist of the components of $\underline{\tau}$ for this model and the remaining entries will be set equal to zero. The same rule applies of course to $\underline{a}^k$.

Since the relative differences between the components of $\underline{\tau}^i$ and the relative ratios between the (nonzero) components of $\underline{a}^i$ remain invariant for a given model i, we form two feature vectors $\underline{\tilde{\tau}}^i$ and $\underline{\tilde{a}}^i$ defined by

$$\underline{\tilde{\tau}}^i = (\tilde{\tau}^i_1, \ldots, \tilde{\tau}^i_M),$$

$$\underline{\tilde{a}} = (\tilde{a}^i_1, \ldots, \tilde{a}^i_M)$$

and

$$\tilde{\tau}^i_k = \tau^i_k - \tau^i_1 + 1 , \qquad \tau^i_k \neq 0$$

$$\tilde{a}^i_k = a^i_k / (0.1 \max_j a^i_j)$$

(where τ^i_k and a^i_k denote the parameters τ_k and a_k for the ith model defined in the preceding sections).

A simulation was performed in which the values of the feature vectors $\underline{\tilde{\tau}}^i$, and $\underline{\tilde{a}}^i$, $i = 1, 2, 3$, for the three models 59, 60, and 66 obtained from clean data in the preceding section (Table 1) were

considered as "trained models".

Then four incoming model signatures were fabricated by adding different amounts of zero mean white Gaussian noise to the signatures of models 59, 60, and 66. Specifically the four models were created with (1) model 59 noisy signature with signal-to-noise S/N = 7.75; (2) same as (1) except that S/N = 1.29; (3) Model 60 noisy signature with S/N = 7.75; and (4) model 66 noisy signature with S/N = 7.75. The values of the feature vectors $\underline{\tilde{\tau}}$ and $\underline{\tilde{a}}$ for each of these signature were calculated by our method.

A nearest neighbor algorithm was used to classify each of the incoming models. For this purpose, the Euclidian distance between the values of the $\underline{\tilde{\tau}}$ vectors was used as the distance measure. For those trained models, for which certain components of the vectors $\underline{\tilde{\tau}}$ were very close, we used the values of the corresponding components of the vector $\underline{\tilde{a}}$ as some of the feature variables (in addition to the delay feature variables mentioned above). This nearest neighbor algorithm classified correctly all the above four incoming signatures.

5. CONCLUSION

The preceding results show that the signal processing of wide bandwidth radar returns by frequency domain Prony methods constitute a very economic way of reducing the dimensionality (extracting features) of the signatures observed, and lead to classification algorithms which are very accurate even in the presence of considerable noise. These developments clearly extend to the case of equations (2) and (3) as discussed in [1].

REFERENCES

1. R. J. P. de Figueiredo and C. L. Hu, "A Fourier-Prony Tauberian Approach to the Analysis of a Mixture of Delayed Signals," Rice University Technical Report EE-7907, Houston, Texas, September 1979.

2. D. O. Cisco, J. K. Johnston and G. W. Gruver, "Radar Signature Investigation Volume I - Measurements Report," RADC-TR-70-257, Volume I of II, Rome Air Development Center, Rome, New York, November 1970.

3. D. O. Cisco, G. P. Coble and G. W. Gruver, "Radar Signature Investigation Volume II - Target Classification," RADC-TR-70-257, Volume II of II, Rome Air Development Center, Rome, New York, November 1970.

4. C. L. Bennett, A. M. Auckenthaler, R. S. Smith and J. D. DeLorenzo, "Space-Time Integral Equation Approach to the Large Body Scattering Problem," RADC-TR-73-70, Rome Air Development Center, Rome, New York, May 1973.

5. P. H. Stockmann, "High-Dimensional Discriminant Analysis of Complex Sampled Data Radar Signals," Ph.D. Dissertation, Electrical and Computer Engineering Department, Syracuse University, Syracuse, New York, June 1973.

6. H. Webb, Private Communication.

7. E. M. Kennaugh, "Estimation and Interpretation of Aircraft Echoing Characteristic for Target Identification Use," Private Communciation, October 1977.